

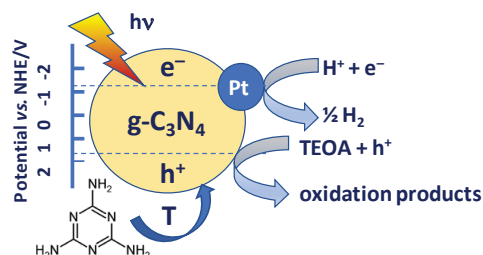
Synthesis of graphitic carbon nitride-based photocatalysts for hydrogen evolution under visible light

Angelina V. Zhurenok, Tatyana V. Larina, Dina V. Markovskaya, Svetlana V. Cherepanova, Elena A. Mel'gunova and Ekaterina A. Kozlova*

Federal Research Center G. K. Boreskov Institute of Catalysis, Siberian Branch of the Russian Academy of Sciences, 630090 Novosibirsk, Russian Federation. Fax: +7 383 324 9543; e-mail: kozlova@catalysis.ru

DOI: 10.1016/j.mencom.2021.03.004

The optimal conditions for the synthesis of platinumized graphitic carbon nitride (Pt/g-C₃N₄) have been found. It was investigated as a catalyst for the production of hydrogen from aqueous solutions of triethanolamine (TEOA) under irradiation with visible light. The highest photocatalytic activity of 450 μmol h⁻¹ g⁻¹ and an apparent quantum efficiency of 1.1% were demonstrated by the 1% Pt/g-C₃N₄ sample prepared from melamine by calcining at 600 °C for 2 h.



Keywords: graphitic carbon nitride, photocatalytic hydrogen evolution, visible light, platinum, heterogeneous catalysis, semiconductors, triethanolamine.

The annual increase in energy consumption and the reduction in the reserves of fossil carbon-containing raw materials necessitate the development of new types of renewable energy sources. Areas of alternative energy based on the use of solar energy are of paramount scientific importance, and in the future, they have significant practical prospects.¹ Special attention is paid to the production of hydrogen by water splitting under visible light in the presence of semiconductor photocatalysts.² The possibility of photocatalytic water splitting to form hydrogen and oxygen was first described by Fujishima and Honda in 1972.³ The discovery of graphitic carbon nitride (g-C₃N₄) polymer gave a new impetus to the development of methods for the synthesis of materials for hydrogen production.⁴ This material is a semiconductor with a band gap energy (E_g) of 2.7 eV ($\lambda = 460$ nm). The energy levels of the valence band and conduction band lie at +1.6 and -1.1 V vs. NHE, respectively.⁵ The latter value is one of the most negative valence band values for known photocatalysts and favors the water reduction process.

Traditionally, g-C₃N₄ is synthesized by thermal condensation of nitrogen-enriched organic precursors – cyanamides, melamine and urea.⁴ However, the photocatalytic activity of g-C₃N₄ synthesized by this method is usually low due to the rapid recombination of photogenerated electron–hole pairs. Various approaches to increasing the activity of photocatalysts based on g-C₃N₄ are being developed. Recently, systems such as CdS/g-C₃N₄,⁶ TiO₂/g-C₃N₄,⁷ BiVO₄/g-C₃N₄⁸ and CoO/g-C₃N₄⁹ have been proposed for hydrogen production. However, the high activity has been previously achieved by simply changing the calcination temperature of the precursor, melamine.¹⁰ Additionally, it is well known that the activity can be enhanced by changing the amount of cocatalyst metal, e.g., Pt.² In this work, we investigated the influence of the photocatalyst synthesis conditions, such as the type of precursor, the mode of heat treatment and the amount of supported Pt, on the rate of

photocatalytic hydrogen evolution from alkaline aqueous solutions of triethanolamine (TEOA).

The synthesis of graphitic carbon nitride was performed by the classical technique – thermal condensation of the precursors, melamine and dicyandiamide. Three variable parameters, viz. the precursor (melamine and dicyandiamide), the heating temperature (from 450 to 600 °C with a constant heating time of 4 h) and the heating time (2 and 4 h at a temperature of 600 °C), were selected to optimize the preparation conditions.[†] Also, 1 or 3% platinum was deposited on the prepared photocatalysts by impregnation with hexachloroplatinic acid, followed by reduction with sodium borohydride.¹¹ Without the addition of platinum, the rate of hydrogen evolution was zero for all samples.

The synthesized samples were analyzed by X-ray diffraction (XRD), UV-VIS spectroscopy and low-temperature N₂ adsorption techniques (Table 1, Figure 1).[†] The XRD patterns of the samples synthesized at 500 and 600 °C are displayed in Figure 1(a). The dominant diffraction peak ($2\theta \sim 27^\circ$) can be attributed to the plane (002) and determines the distance between the 2D layers of the graphitic carbon nitride.⁴ The second peak, located at $2\theta \sim 13$, is due to the distance between the tri-s-triazine units within the 2D layer.⁴ According to Table 1, the average crystallite size in the direction perpendicular to the 2D layers (L_c) increases significantly with the calcination temperature, which indicates the ordering of the layer structure, whereas the average crystallite size in the plane of the layers (L_a) slightly decreases. For samples synthesized from melamine, L_a is higher than that for g-C₃N₄ obtained from dicyandiamide. If we compare the samples calcined at 600 °C for 2 and 4 h for both precursors, melamine and dicyandiamide, the interplanar distances d_{002} and d_{100} decrease with an increase in the calcination time, which means a higher crystallinity of

[†] For details, see Online Supplementary Materials.

Table 1 Structural characteristics of the g-C₃N₄ samples determined from XRD patterns.

Sample	Precursor	T/°C	Heating time/h	d ₁₀₀ /Å	d ₀₀₂ /Å	L _a /nm ^a	L _c /nm ^b
C ₃ N ₄ -M (500 °C 4h)	Melamine	500	4	6.74	3.28	7.6	5.0
C ₃ N ₄ -M (600 °C 2h)	Melamine	600	2	6.80	3.25	4.6	9.0
C ₃ N ₄ -M (600 °C 4h)	Melamine	600	4	6.70	3.23	5.0	8.9
C ₃ N ₄ -D (500 °C 4h)	Dicyandiamide	500	4	6.72	3.27	6.8	4.7
C ₃ N ₄ -D (600 °C 2h)	Dicyandiamide	600	2	6.82	3.27	5.3	7.6
C ₃ N ₄ -D (600 °C 4h)	Dicyandiamide	600	4	6.73	3.24	5.1	7.6

^a Average crystallite size in the plane of the layer. ^b Average crystallite size in the direction perpendicular to the layer.

the material, in other words, a tighter packing of polymer layers and enhancing the conjugation on the tri-s-triazine units.¹²

The surface area of the photocatalysts increases significantly with calcination temperature [Figure 1(b)]. At temperatures from 450 to 500 °C, the specific surface area of the synthesized samples is below 10 m² g⁻¹, while starting with 550 °C, it increases up to 13–28 m² g⁻¹. Note that the surface area of g-C₃N₄ synthesized from melamine generally exceeds that for g-C₃N₄ from dicyandiamide. UV-VIS spectra of the samples were measured [Figure 1(c)], and the Tauc plots were obtained [Figure 1(d)]. One can see that the band gap energy decreases slightly with an increase in the calcination temperature, while the lowest E_g value of ca. 2.8 eV is observed for the g-C₃N₄ sample prepared from melamine (600 °C, 2 h).

The photocatalytic hydrogen evolution from alkaline (0.1 M NaOH) aqueous solutions of TEOA (10 vol%) under irradiation with visible light (λ = 450 nm) was investigated. TEOA was used as a sacrificial reagent in the reaction system. This substrate can protect the photocatalyst surface from photocorrosion and react with the photogenerated holes improving charge separation and catalytic activity.¹³ In the preliminary experiments, it was shown that the addition of alkali increases the reaction rate by an order of magnitude. The experimental setup is described in detail elsewhere^{14,15} and in Online Supplementary Materials.

Platinized samples were examined using high-resolution transmission electron microscopy, and platinum (marked in yellow in Figure S2[†]) was detected as nanoparticles 5–10 nm in

size. The effect of the amount of added platinum on the rate of photocatalytic hydrogen evolution was estimated. The addition of 1 wt% platinum has been shown to result in higher activity compared to 3 wt% deposited metal [Figure 2(a)]. When the metal concentration is high, the deposited cocatalyst can scatter incident light and reduce light absorption. It is also known that an excess amount of metal cocatalysts plays the role of recombination centers.¹⁶ The effect of calcination temperature [Figure 2(b)] and calcination time [Figure 2(c)] on activity was considered. First, the calcination temperature was changed from 450 to 600 °C with a constant calcination time of 4 h. The results obtained should be discussed taking into account the mechanism of g-C₃N₄ formation (Figure S3[†]). At the first stage, melamine was formed from dicyandiamide, after which it was transformed into melom and melom.¹⁷ The next stage of the process was the polymerization of melom with the formation of the target g-C₃N₄ material.¹⁷ It was noted that the latter reaction proceeded with sufficient yield if the temperature was above 520 °C.¹⁷ The obtained kinetic data showed that the samples synthesized at temperatures from 450 to 500 °C have a very low photocatalytic activity, up to 0.01 μmol min⁻¹, which is probably due to the very low specific surface area and the yield of the polymerization reaction. At temperatures from 550 to 600 °C, the yield of g-C₃N₄ increases, the surface area of the samples becomes 10–20 m² g⁻¹, and the rate of hydrogen evolution reaches higher values. Raising the heating temperature leads to increase in the degree of decomposition of the precursors as well as the

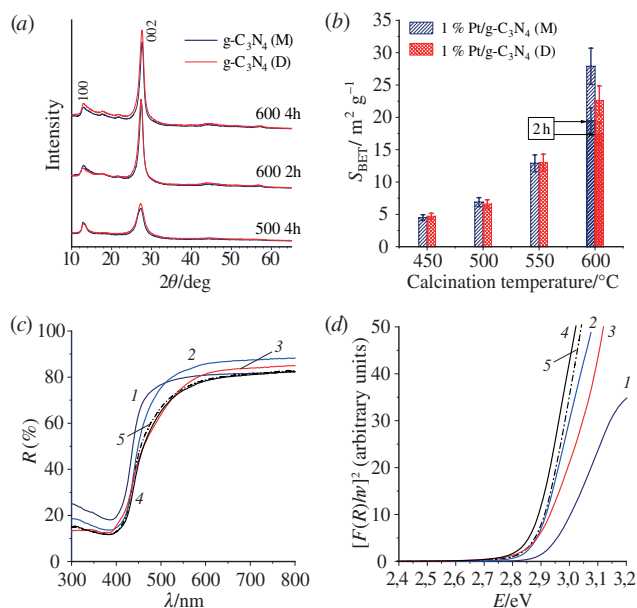


Figure 1 (a) XRD patterns of g-C₃N₄ samples and (b) surface area of 1% Pt/g-C₃N₄ samples prepared from melamine and dicyandiamide under various conditions; (c) UV-VIS spectra and (d) Tauc plots for g-C₃N₄ samples prepared from melamine at (1) 500, (2) 550 and (3) 600 °C for 4 h and (4) at 600 °C for 2 h, and also (5) from dicyandiamide at 600 °C for 2 h.

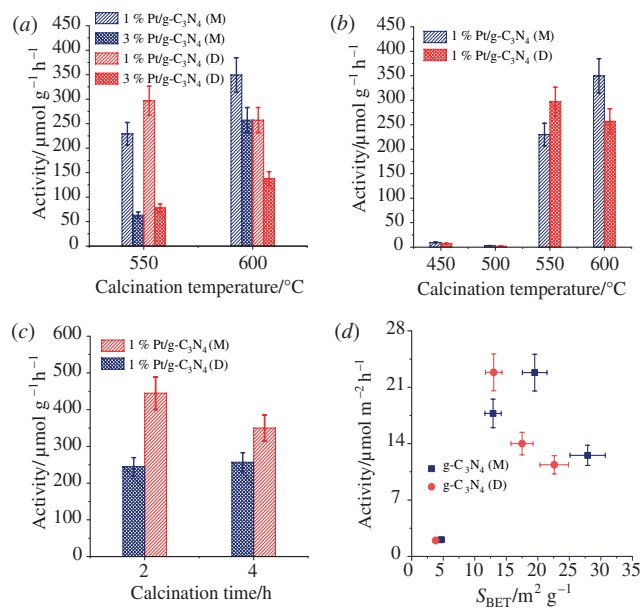


Figure 2 Dependences of the hydrogen evolution rate on (a) the platinum content, (b) the calcination temperature and (c) the calcination time and (d) the dependence of the catalytic activity normalized to S_{BET} on S_{BET} when using photocatalysts obtained from melamine (M) and dicyandiamide (D).

Table 2 Influence of synthesis conditions on the properties of 1% Pt/g-C₃N₄ photocatalyst for photocatalytic hydrogen evolution.^a

Precursor	Synthesis conditions		$S_{\text{BET}}/\text{m}^2 \text{g}^{-1}$	$W(\text{H}_2)^b/\mu\text{mol min}^{-1}$	Catalytic activity/ $\mu\text{mol g}^{-1} \text{h}^{-1}$	Catalytic activity/ $\mu\text{mol m}^{-2} \text{h}^{-1}$
	$T/^\circ\text{C}$	Heating time/h				
Melamine	450	4	< 10	< 0.01	< 10	< 1
Dicyandiamide	450	4	< 10	< 0.01	< 10	< 1
Melamine	500	4	< 10	< 0.01	< 10	< 1
Dicyandiamide	500	4	< 10	< 0.01	< 10	< 1
Melamine	550	4	12.9	0.191	229	17.8
Dicyandiamide	550	4	13.0	0.247	297	22.8
Melamine	600	4	27.9	0.291	350	12.5
Dicyandiamide	600	4	22.6	0.214	257	11.4
Melamine	600	2	19.5	0.371	445	22.8
Dicyandiamide	600	2	17.5	0.204	245	14.0

^a Catalytic tests were carried out in alkaline (0.1 M NaOH) aqueous solutions of TEOA under irradiation with visible light at a wavelength of 450 nm.

^b The rate of hydrogen evolution.

crystallinity and, consequently, the photocatalytic activity of resulting g-C₃N₄. A further increase in the calcination temperature is not reasonable due to the low thermal stability of the material above 600 °C.¹⁷ Thus, the optimal temperature of precursor calcination is 600 °C. Second, for further optimization of the synthesis, the samples were obtained at different calcination times, 2 and 4 h, at 600 °C. Experiments have shown that the optimal conditions for the preparation of g-C₃N₄ are the annealing of melamine at 600 °C for 2 h [Figure 2(c)]. Melamine is a better precursor than dicyandiamide, most likely due to the larger surface area of g-C₃N₄ formed. However, as shown in Figure 2(d), the hydrogen evolution rate does not linearly depend on the specific surface area. The high activity of the photocatalyst 1% Pt/g-C₃N₄ (melamine, 600 °C, 2 h) may be due to the optimal values of interplanar distance, crystallite size and E_g . The obtained values of catalytic activity exceed those published recently (Table S2[†]). Note that a decrease in the average size of g-C₃N₄ crystallites in the plane of the layer (L_a) leads to an increase in the reaction rate. The small particle size likely facilitates the diffusion and separation of photogenerated charge carriers in space, which improves catalytic activity. The optimal value of L_a is ca. 5 nm.

In conclusion, the procedure for the synthesis of g-C₃N₄ has been optimized, and for the first time, the factors influencing the catalytic activity, such as the nature of the precursor, the temperature and duration of calcination and the amount of co-catalyst, have been comprehensively studied. The most active sample, 1% Pt/g-C₃N₄, was prepared from melamine by calcining at 600 °C for 2 h and demonstrated a catalytic activity of 450 $\mu\text{mol H}_2 \text{h}^{-1} \text{g}^{-1}$ and an apparent quantum efficiency of 1.1%. The resulting activity value exceeds those recently published for this system type.¹⁸

This work was supported by the Russian Foundation for Basic Research (project no. 20-33-70086). Authors thank Dr. E. Yu. Gerasimov for TEM investigations.

Online Supplementary Materials

Supplementary data associated with this article can be found in the online version at doi: 10.1016/j.mencom.2021.03.004.

References

- 1 A. Kubacka, M. Fernández-García and G. Colón, *Chem. Rev.*, 2012, **112**, 1555.
- 2 E. A. Kozlova and V. N. Parmon, *Russ. Chem. Rev.*, 2017, **86**, 870.
- 3 A. Fujishima and K. Honda, *Nature*, 1972, **238**, 37.
- 4 X. Wang, K. Maeda, A. Thomas, K. Takanabe, G. Xin, J. M. Carlsson, K. Domen and M. Antonietti, *Nat. Mater.*, 2009, **8**, 76.
- 5 S. Ye, R. Wang, M.-Z. Wu and Y.-P. Yuan, *Appl. Surf. Sci.*, 2015, **358**, 15.
- 6 H. He, J. Cao, M. Guo, H. Lin, J. Zhang, Y. Chen and S. Chen, *Appl. Catal., B*, 2019, **249**, 246.
- 7 J. Yan, H. Wu, H. Chen, Y. Zhang, F. Zhang and S. F. Liu, *Appl. Catal., B*, 2016, **191**, 130.
- 8 Z. Qin, W. Fang, J. Liu, Z. Wei, Z. Jiang and W. Shangguan, *Chin. J. Catal.*, 2018, **39**, 472.
- 9 F. Guo, W. Shi, C. Zhu, H. Li and Z. Kang, *Appl. Catal., B*, 2018, **226**, 412.
- 10 M. Caux, F. Fina, J. T. S. Irvine, H. Idriss and R. Howe, *Catal. Today*, 2017, **287**, 182.
- 11 E. A. Kozlova, T. P. Lyubina, M. A. Nasalevich, A. V. Vorontsov, A. V. Miller, V. V. Kaichev and V. N. Parmon, *Catal. Commun.*, 2011, **12**, 597.
- 12 Q. Gu, Z. Gao, H. Zhao, Z. Lou, Y. Liao and C. Xue, *RSC Adv.*, 2015, **5**, 49317.
- 13 V. Kumaravel, M. D. Imam, A. Badreldin, R. K. Chava, J. Y. Do, M. Kang and A. Abdel-Wahab, *Catalysts*, 2019, **9**, 276.
- 14 A. V. Stavitskaya, E. A. Kozlova, A. Yu. Kurenkova, A. P. Glotov, D. S. Selischev, E. V. Ivanov, D. V. Kozlov, V. A. Vinokurov, R. F. Fakhruddin and Yu. M. Lvov, *Chem. – Eur. J.*, 2020, **26**, 13085.
- 15 E. A. Kozlova, A. Yu. Kurenkova, E. Yu. Gerasimov, N. V. Gromov, T. B. Medvedeva, A. A. Saraev and V. V. Kaichev, *Mater. Lett.*, 2021, **283**, 128901.
- 16 D. Vasilchenko, P. Topchiyan, A. Tsygankova, T. Asanova, B. Kolesov, A. Bukhtiyarov, A. Kurenkova and E. Kozlova, *ACS Appl. Mater. Interfaces*, 2020, **12**, 48631.
- 17 Y. Zheng, L. Lin, B. Wang and X. Wang, *Angew. Chem., Int. Ed.*, 2015, **54**, 12868.
- 18 M. Inagaki, T. Tsumura, T. Kinumoto and M. Toyoda, *Carbon*, 2019, **141**, 580.

Received: 30th November 2020; Com. 20/6382